

Multi-frequency harmonic arrays: initial experience with a novel transducer concept for nonlinear contrast imaging

Flemming Forsberg^{a,*}, William T. Shi^{a,1}, Bahram Jadidian^{b,2}, Alan A. Winder^{c,2}

^a Department of Radiology, Division of Ultrasound, Thomas Jefferson University, Suite 763J, Main Building, 132 South 10th Street, Philadelphia, PA 19107, USA

^b Layered Manufacturing Inc., New Brunswick, NJ 08901, USA

^c Acoustic Sciences Associates, Westport, CT 06880, USA

Received 12 February 2004; received in revised form 12 April 2004; accepted 14 April 2004

Available online 10 May 2004

Abstract

Nonlinear contrast imaging modes such as second harmonic imaging (HI) and subharmonic imaging (SHI) are increasingly important for clinical applications. However, the performance of currently available transducers for HI and SHI is significantly constrained by their limited bandwidth. To bypass this constraint, a novel transducer concept termed multi-frequency harmonic transducer arrays (MFHA's) has been designed and a preliminary evaluation has been conducted. The MFHA may ultimately be used for broadband contrast enhanced HI and SHI with high dynamic range and consists of three multi-element piezo-composite sub-arrays (A–C) constructed so the center frequencies are $4f_A = 2f_B = f_C$ (specifically 2.5/5.0/10.0 MHz and 1.75/3.5/7.0 MHz). In principle this enables SHI by transmitting on sub-array C receiving on B and, similarly, from B to A as well as HI by transmitting on A receiving on B and, likewise, from B to C. Initially transmit and receive pressure levels of the arrays were measured with the elements of each sub-array wired in parallel. Following contrast administration, preliminary in vitro HI and SHI signal-to-noise ratios of up to 40 dB were obtained. In conclusion, initial design and in vitro characterization of two MFHA's have been performed. They have an overall broad frequency bandwidth of at least two octaves. Due to the special design of the array assembly, the SNR for HI and SHI was comparable to that of regular B-mode and better than commercially available HI systems. However, further research on multi-element MFHA's is required before their potential for in vivo nonlinear contrast imaging can be assessed. © 2004 Elsevier B.V. All rights reserved.

Keywords: Transducer design; Transducer arrays; Ultrasound contrast agent; Harmonic imaging; Subharmonic imaging

1. Introduction

Over the past decade, a number of microbubble-based ultrasound contrast agents have been developed [1]. Such agents are capable of enhancing Doppler ultrasound signal intensities and, in some cases also grayscale echogenicity. Moreover, the microbubbles act as nonlinear oscillators producing significant energy components in the received echo signals, which

span the range of possible frequency emissions from subharmonics through ultraharmonics [1,2]. These nonlinear bubble echoes can be separated from tissue echoes and used to create second harmonic imaging (HI) and subharmonic imaging (SHI), which allow blood flow in small or even capillary blood vessels surrounded by moving tissue (e.g., myocardial perfusion) to be detected [1].

HI has been extensively studied [3–6], since the intensity of the second harmonic signals is generally greater than that of the subharmonic, and this imaging mode is commercially available. However, HI suffers from reduced blood-to-tissue contrast resulting from second harmonic generation and accumulation in tissue, which makes SHI an attractive alternative because subharmonic signals are not generated in tissue (at diagnostic pressures and frequencies) and some new

* Corresponding author. Tel.: +1-215-955-4870; fax: +1-215-955-8549.

E-mail address: flemming.forsberg@jefferson.edu (F. Forsberg).

¹ Current address: GE Medical Systems, Milwaukee, WI 53201, USA.

² Current address: J&W Medical LLC, Westport, CT 06880, USA.

contrast agents produce significant subharmonic scattering. Although, the magnitude of the subharmonic signal intensity in tissues is much smaller than that of the second harmonic [7], SHI should have better lateral resolution and may cause less cavitation bioeffects due to the higher transmitting frequency. Feasibility studies of SHI have been conducted in vitro and in vivo by our group [8–10] and by others [7,11].

However, the performance of currently available transducers for HI and SHI is significantly constrained by their limited bandwidth. Hence, we have developed and performed a preliminary evaluation of a new multi-frequency (fundamental, subharmonic and second harmonic) transducer array designed for broadband ultrasound contrast imaging with high dynamic range (although this initial study did not involve a transducer configuration suitable for imaging). Such a multi-frequency harmonic transducer array (MFHA) promises to increase the performance of ultrasound contrast imaging in current applications and permit new uses that exploit the nonlinear properties of contrast microbubbles.

2. Transducer design and fabrication

Two MFHA's consisting of three multi-element piezo-composite sub-arrays (A–C) were constructed with center frequencies $4f_A = 2f_B = f_C$ (2.5/5.0/10.0 and 1.75/3.5/7.0 MHz, respectively). This enabled SHI by transmitting on sub-array C receiving on B and, similarly, from B to A as well as HI by transmitting on A receiving on B and, likewise, from B to C. The frequencies were selected to cover the ranges used in echocardiography and deep abdominal imaging (i.e., 1.75 and 2.5 MHz) as well as in more superficial imaging applications (i.e., for $f > 5$ MHz).

The sub-arrays were produced using a layered manufacturing technology, namely fused deposition of ceramics (FDC) process [12,13]. In the FDC process, solid objects are built layer by layer from ceramic loaded thermoplastic filaments by using computer-aided design (CAD) software programs. A flexible filament of the ceramic–polymer mixture is fed by a pair of counter rotating rollers into a dispensing head that includes a liquifier and nozzle outlet. Inside the liquifier, the filament softens and melts at a temperature just above its melting point. As the counter-rotating rollers continue to advance the solid filament into the liquifier, the force of the incoming solid filament extrudes the molten material out from the nozzle where it is deposited on a build platform position in close proximity to the dispensing head. The CAD software controls the movement of the dispensing head in the horizontal X – Y plane and controls the movement of the build platform in the Z direction (Fig. 1), leading to the creation of an object that is a three-dimensional depiction of the CAD model.

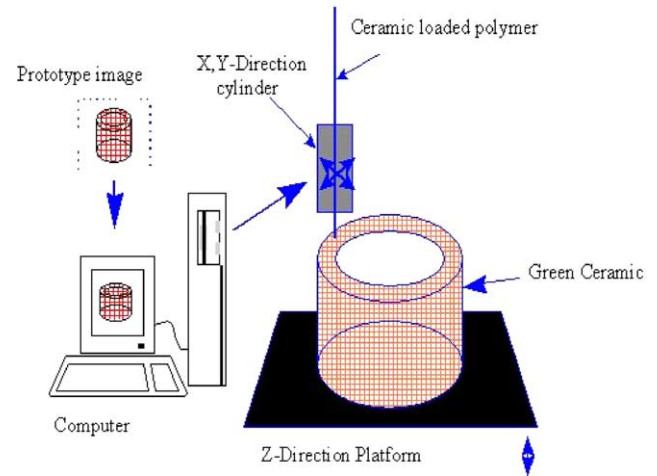


Fig. 1. Schematic of the FDC process.

The transducer fabrication approach was based on extruding continuous PZT feed filaments with high solid loading (≈ 55 vol%). PZT-5H (TRS600; TRS Ceramics Inc., State College, PA) powder was initially coated with stearic acid, compounded with a binder formulation (developed at Rutgers University) in a high shear mixer, and then fed into a single screw extruder to make a flexible filament 1.75 mm in diameter. A solid three-dimensional model (CAD file) of the linear piezoceramic–composite arrays (with 2–2 connectivity) was designed and the part(s) made using the FDC process. To build sub-arrays with various resonance frequencies, different nozzle sizes were used to deposit ceramic elements of appropriate width and kerf sizes, as shown in Table 1.

The binder was removed by slow heating to 550 °C, followed by a bisque firing at 780 °C to give enough mechanical strength to the ceramic parts for further handling and assembly. Sintering was carried out at 1285 °C for 1 h, after which the average density of the ceramic samples was 7.7 g/cm³ and the longitudinal, transversal and thickness shrinkages were 18%, 16% and 19%, respectively. The sintered structures were embedded in epoxy (Epotek 301 with a density of 1.01 g/cm³; Epoxy Technology, Billerica, MA) and cured overnight at room temperature. The sub-array composites were then polished to proper thickness, electroded using silver epoxy (4929N, Silver Composition; DuPont Electronics, Wilmington, DE), and poled in an oil bath at 60 °C for 5 min under 20 kV/cm electric field. The ceramic volume percent of the composites, V_{cer} , was determined by:

$$V_{\text{cer}} = \frac{(\rho_{\text{com}} - \rho_{\text{pol}})}{(\rho_{\text{cer}} - \rho_{\text{pol}})} \times 100\% \quad (1)$$

where ρ_{com} , ρ_{pol} and ρ_{cer} are the densities of composite, Epotek 301 epoxy, and the bulk PZT ceramic, respectively.

Table 1
FDC fabrication process parameters

Resonance frequency (MHz)	Theoretical		Actual		Nozzle diameter (μm)	Ceramic width deposited (μm)	Composite thickness (μm)
	Ceramic width (μm)	Polymer Kerf (μm)	Ceramic width (μm)	Polymer Kerf (μm)			
2.5	360	440	360	450	400	425	600
5	180	220	180	230	200	225	300
10	100	110	100	120	100	125	150
1.75	500	400	490	415	575	600	860
3.5	250	200	240	215	275	300	430
7.0	125	100	115	120	125	150	215

After 24 h aging, the dielectric and piezoelectric properties of the elements were evaluated. Assuming a free-air resonator, the clamped capacitance of the sub-array composites, C_p , was measured at 1 kHz using an RLC Digibridge (model 1689M, GenRad Inc., Concord, ME). The relative dielectric constant, K , and the piezoelectric voltage coefficient, g_{33} were then calculated using the following equations:

$$K = \frac{C_p t}{\epsilon_0 A} \quad (2)$$

$$g_{33} = \frac{d_{33}}{\epsilon_0 K} \quad (3)$$

where t is the thickness of the samples, A is the electrode area, and ϵ_0 is the permittivity of vacuum (8.854×10^{-12} F/m). The piezoelectric charge coefficient, d_{33} , of the composites was measured at 100 Hz by a Berlincourt Piezometer (Channel Products Inc., Chesterland, OH) using two flat probes. The resonance and antiresonance frequencies (f_s and f_p , respectively) were obtained from an impedance plot using an HP 4194A impedance analyzer (Hewlett Packard, Santa Clara, CA) allowing the thickness coupling coefficient of the composites, k_t , to be determined as:

$$k_t^2 = \frac{\pi f_s}{2 f_p} \tan \left(\frac{\pi f_p - f_s}{f_p} \right) \quad (4)$$

as shown in Table 2.

A matching layer with an acoustic impedance of 3.9 MRayls was used to approximate the optimum acoustic impedances of the matching layers (calculated utilizing the Mason model for an air-backed equivalent circuit [14]). The matching layer was prepared by mixing solid spherical glass powder (2.5 μm in diameter) and Spurr epoxy (Ernest F. Fullam Inc., Latham, NY) in a volume ratio of 35–65%, respectively [15]. The matching layers (ranging in thickness from 38.5 to 220 μm ; Table 2) were attached on the front face of each sub-array by a thin layer (<2 μm) of Spurr epoxy.

The first MFHA was based on the design criterion of making the length of each sub-array almost equal to achieve uniform element sensitivity. This was accomplished by doubling the number of elements as the resonant frequency in the thickness mode was doubled, increasing the number of elements from 8 to 16 to 32. However, the sub-arrays were unfocussed and thus had a pressure maximum at the $L^2/4\lambda$ point on their maximum response axis, where L is the overall active length of each sub-array (Table 2). The 2.5 MHz sub-array, therefore, was on the decaying portion of its axial

Table 2
Physical and electromechanical properties of the MFHA's

Property	2.5 MHz	5.0 MHz	10.0 MHz	1.75 MHz	3.5 MHz	7.0 MHz
Number of elements	8	16	32	15	21	29
Element width (μm)	810	410	220	905	455	235
Active length (mm)	6.03	6.33	6.92	13.57	9.56	6.81
Density (g/cm^3)	4.12	4.09	4.19	4.84	4.80	7.72
Ceramic volume fraction V_{cer} (%)	44	44	45	55	54	53
Charge coefficient d_{33} (pC/N)	350	340	340	340	340	360
Dielectric constant	847	851	586	785	884	801
Dissipation factor ($\tan \delta$) @ 1 kHz	0.023	0.022	0.031	0.021	0.020	0.020
Coupling factor k_t (%)	66.8	67.3	60.6	71	63	66
Voltage coefficient g_{33} (10^{-3} V m/N)	46.7	45.1	65.5	48.9	43.4	50.8
Velocity of sound (m/s)	2946	3228	3004	2886	2881	2607
Acoustic impedance Z (MRayls)	12.14	13.19	12.59	13.96	13.82	12.30
Matching layer thickness (μm)	154.0	77.0	38.5	220.0	110.0	55.0
Capacitance @ resonance frequency (pF)	243	494	730	331	527	674

response at the mechanical focus of the MFHA (i.e., at 50 mm) and beyond its -6 dB depth of field. However, the 50 mm focus was within the depth of field of the 5.0 and 10.0 MHz sub-arrays. Alternatively, the 1.75/3.5/7.0 MHz array was designed based on making the focal point of each array equal to the mechanical focus, of 50 mm (with 15, 21 and 29 elements, respectively). After several iterations, it was decided to omit a backing layer in this initial design and opt for an increase in sensitivity by using air-backed arrays instead.

Finally, the complete prototype assembled MFHA's, with all elements of each sub-array wired in parallel (to increase sensitivity), were placed in a waterproof housing with a fixed mechanical curvature of 50 mm. The relative azimuthal positions of the sub-arrays on the concave surface were selected to minimize the cross-correlation function between the sub-arrays (i.e., minimizing inter-sub-array spatial correlation). The dielectric constant ranged from 586 to 851 for the 2.5/5.0/10.0 MFHA and from 785 to 884 for the 1.75/3.5/7.0 array (Table 2). In both MFHAs the coupling factors achieved were above 60%.

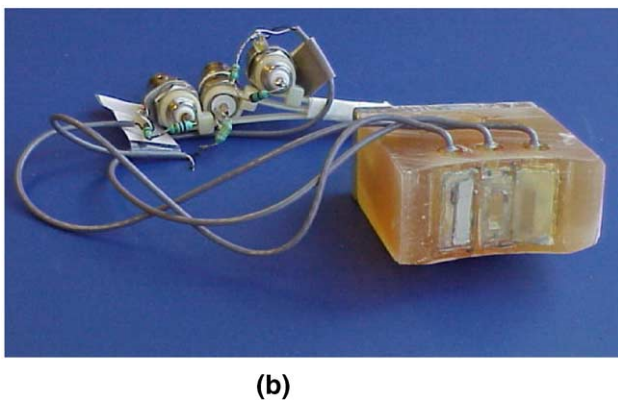
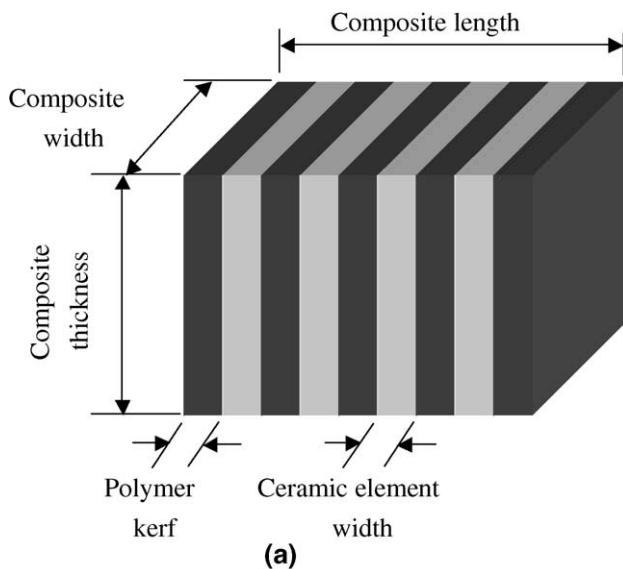


Fig. 2. Schematic of the sub-array composites (a) and photo of MFHA in housing (b), with mechanical curvature of 50 mm.

A schematic of the sub-array composites and a photo of one of the two multi-frequency array configurations that was fabricated for testing are shown in Fig. 2. While the lack of a backing layer and the elements wired in parallel increase sensitivity, it clearly also makes these MFHA configurations unsuitable for imaging (as does the fixed mechanical focus). However, for this initial evaluation the intention was only to provide a proof-of-concept for the MFHA design.

3. Acoustic characterization

The MFHA was placed in a water-bath (≈ 1.0 l of distilled water) and a programmable function generator (Model 8116A; Hewlett Packard, Santa Clara, CA) was used to produce 16 cycle tone bursts for transmission. The transmit signals were first amplified in a broadband 50 dB RF power amplifier (Model 325LA; ENI, Rochester, NY) and then supplied to the MFHA assembly with the corresponding sub-arrays. The transmitting sensitivities of the sub-arrays were measured along the axis of maximum response at field points from 1 to 6 cm. Acoustic pressure was determined using a calibrated, 0.5 mm broadband, acoustic needle hydrophone (Precision Acoustics, Inc., Dorchester, UK) by varying the input frequencies (from 1 to 15 MHz for the same excitation level of 250 mV).

The traditional transmitting response per volt (TRV) is defined at 1 mm from the face of the transmit element. The TRV (unit: kPa/V) was computed as:

$$\text{TRV} = (V_r/V_{in})(\text{TL}/\text{RRS}_{\text{cal}}) \quad (5)$$

where V_r is the output voltage of the calibrated hydrophone at the given field point, V_{in} is the driving voltage to each array, TL is the total one-way transmission loss from the sub-array to the field point (a dimensionless number ≥ 1 which is a function of ultrasonic absorption and spreading losses with distance), and RRS_{cal} (unit: V/kPa) is the sensitivity of the calibrated hydrophone. The sources of absorption in fluids are heat conduction and viscosity, where the contribution of the former is negligibly small for water. The spreading loss is a function of the geometry and boundaries of the propagating medium and may also include diffraction effects.

The pressure levels obtained from 1 to 15 MHz at the mechanical focus (i.e., at an axial distance of 5.0 cm) are presented in Fig. 3a for the 2.5/5.0/10.0 MHz and from 1 to 9 MHz in Fig. 3b for the 1.75/3.5/7.0 MHz sub-array. The MFHA's resonate around the designed center frequencies, although the highest frequency sub-arrays in both cases have a secondary peak around the middle frequency (i.e., f_B). The axial beam profiles along the maximum response axis (MRA) at 2.5, 5.0 and 10.0 MHz are presented in Fig. 4 for the 2.5/5.0/10.0 MFHA.

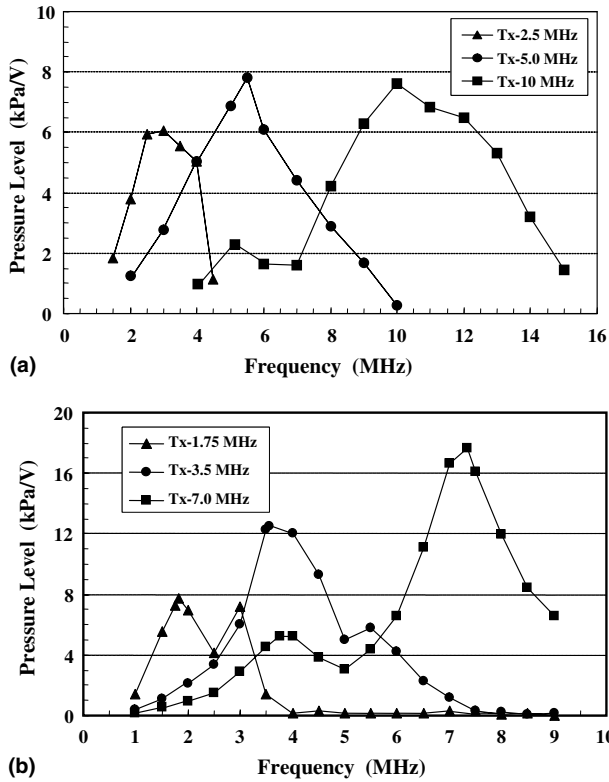


Fig. 3. Transmitting spectral response of (a) the 2.5/5.0/10.0 MHz array and (b) the 1.75/3.5/7.0 MHz array at the mechanical focus of 50 mm.

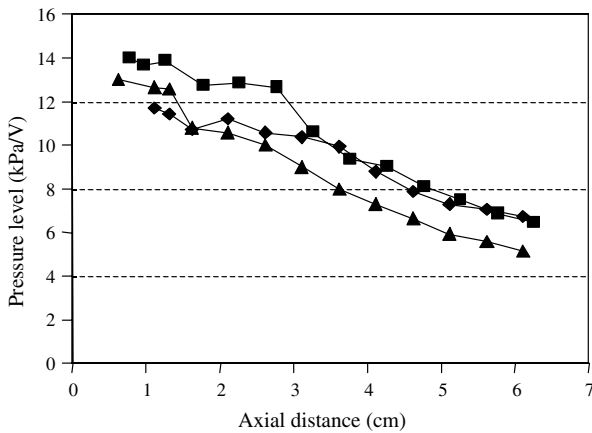


Fig. 4. The axial beam profiles along the MRA for the 2.5 MHz (▲), the 5.0 MHz (■) and the 10.0 MHz (◆) sub-array.

The MRA was determined at two distances (4 and 6 cm) from the transducer surface by adjusting the position of the hydrophone across the ultrasound beam of each sub-array until maximum hydrophone output was achieved. As expected, the pressure level decreases with axial distance, from 12.9 kPa/V (at 0.6 cm) to 5.9 kPa/V at 5.1 cm for the 2.5 MHz sub-array, from 14.0 kPa/V (at 0.8 cm) to 7.5 kPa/V at 5.3 cm for the 5.0 MHz sub-array,

Table 3

Transmit and receive sensitivities for the 2.5/5.0/10.0 MFHA

	2.5 MHz	5.0 MHz	10.0 MHz
TRV (kPa/V) at 1.0 mm	13	13	12
Pressure (kPa/V) at 50 mm	5.9	6.9	7.6
RRS (V/kPa) at face of array	0.0051	0.0067	0.0088

and from 11.7 kPa/V (at 1.1 cm) to 7.3 kPa/V at 5.1 cm for the 10 MHz sub-array, respectively.

The receiving response sensitivities (RRS; unit: V/kPa) of the arrays were measured with a ‘perfect’ reflector (a 10 mm flat steel plate) placed at the mechanical focus (parallel to each sub-array). The RRS is defined as:

$$RRS = (V_r/V_{in})(2TL/[TS \times TRV]) \tag{6}$$

where V_r is the received voltage measured at the output of the sub-array, V_{in} is the driving voltage to each array, and TS is the target strength of the reflector, defined as the echo intensity level at a reference distance of 1 cm from the target, relative to the level of the signal incident on the target. Moreover, TRV is the transmitting response per volt (1 mm from the face of the transmit element) and TL is the total one-way transmission loss from the sub-array to the field point.

From Fig. 4 it can be seen that the TRV’s are flattened near the array faces within 1.5 cm from the transducer surface. This suggests that the TRV 1.0 mm from the array face can be calculated as the TRV approximately 1.0 cm from the array face. Adopting this assumption for the 2.5/5.0/10.0 MHz MFHA, RRS’s (at the mechanical focus of 5.0 cm) were 5.1, 6.7 and 8.8 mV/kPa at 2.5, 5.0 and 10.0 MHz, respectively (Table 3). Pressure sensitivity levels and TRV’s at the mechanical focus are also given in Table 3. The three sub-arrays have minimal intra-array response variability over two octaves; <0.5 dB on transmit and 1.2 dB on receive, which is compatible with commercially available arrays [16]. For the sake of brevity, the corresponding results from the other MFHA have been omitted.

4. In vitro harmonic and subharmonic imaging

The MFHA’s were tested in vitro for HI and SHI using the ultrasound contrast agent Sonazoid® (Amersham Health, Oslo, Norway). Sonazoid is a lipid stabilized suspension of perfluorobutane microbubbles with a median diameter between 2.4 and 3.5 μm and has an excellent harmonic and subharmonic response to ultrasound pulses [9,17]. The finished product of Sonazoid is a powder for reconstitution before injection. After addition of 2 ml of sterile water for injection and gentle shaking by hand the product is easily reconstituted and produces a homogenous dispersion of microbubbles (in

this form the agent is stable for 4 h at room temperature).

For these measurements, the mechanical focus of the MFHA (at 5.0 cm) was placed approximately 2 mm beyond an acoustic window (latex, 12 μm in thickness) on the wall of a 200 ml test chamber placed in the larger water-bath. The Isoton II saline in the test chamber was kept in circulation with a magnetic stirrer. For each measurement, 0.1 ml of reconstituted Sonazoid was injected into the test chamber. Sinusoidal tonebursts of the same length (i.e., of the same acoustic power) were transmitted (using the function generator and amplifier mentioned previously) with 32 cycles (2.5 MHz), 64 cycles (5.0 MHz) and 128 cycles (10.0 MHz) for the 2.5, 5.0 and 10.0 MHz sub-arrays, respectively. For the 1.75/3.5/7.0 MFHA 64 cycle sinusoidal tonebursts were used (i.e., different pulse lengths for the different sub-arrays). As this initial evaluation involved MFHA configurations that were not suitable for imaging, it was decided to use quite long pulse lengths (>32 cycles) to improve the spectral resolution and, thus, the separation between harmonic signals.

Signals scattered from contrast microbubbles were received by the sub-arrays and then amplified with a low noise, 40 dB RF amplifier (Model 5052 PR; Parametrics, Waltham, MA). The amplified signals were sampled at 25 MHz using a digital oscilloscope equipped with mathematical functions (Model 9350AM; LeCroy, Chestnut Ridge, NY). For each measurement, sixty-four received signals were acquired at a pulse repetition frequency of 10 Hz and an averaged spectrum obtained using a Hamming windowed FFT (in the oscilloscope). Finally, the averaged spectrum was transferred via an IEEE-488 interface to a PC for further analysis. Each measurement took less than 10 seconds. The command delivery to the function generator and the data transfer from the digital oscilloscope were controlled by Lab-View[®] (National Instruments, Austin, TX).

Spectra of scattered signals obtained in vitro from Sonazoid microbubbles with the 1.75/3.5/7.0 MFHA operating in HI mode are presented in Fig. 5a and b for 1.75 and 3.5 MHz transmission, respectively. Acoustic pressure amplitudes for the transmitted 1.75 and 3.5 MHz tonebursts were 0.12 and 0.20 MPa, respectively. Strong second harmonic peaks at 3.5 and 7.0 MHz were seen (in Fig. 5a and b, respectively) with high signal-to-noise ratios (SNR's) of around 40 dB. Likewise, spectra from Sonazoid microbubbles acquired with the same 1.75/3.5/7.0 MFHA operating in SHI mode are presented in Fig. 6. Acoustic pressures of 0.39 and 0.40 MPa were used for the transmitted 3.5 and 7.0 MHz tonebursts. High SNR's of around 26 and 34 dB can be seen for the subharmonic components at 1.75 and 3.5 MHz (Fig. 6a and b, respectively). Very similar results were obtained with the 2.5/5.0/10.0 MFHA, but the results have been omitted for the sake of brevity.

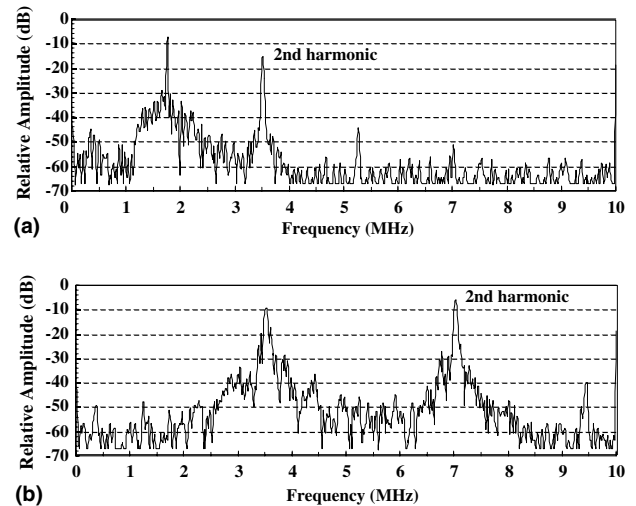


Fig. 5. Spectra from Sonazoid obtained using (a) the 1.75/3.5 MHz sub-arrays for transmission/reception and (b) the 3.5/7.0 MHz sub-arrays for transmission/reception (i.e., the MFHA is operating in HI mode).

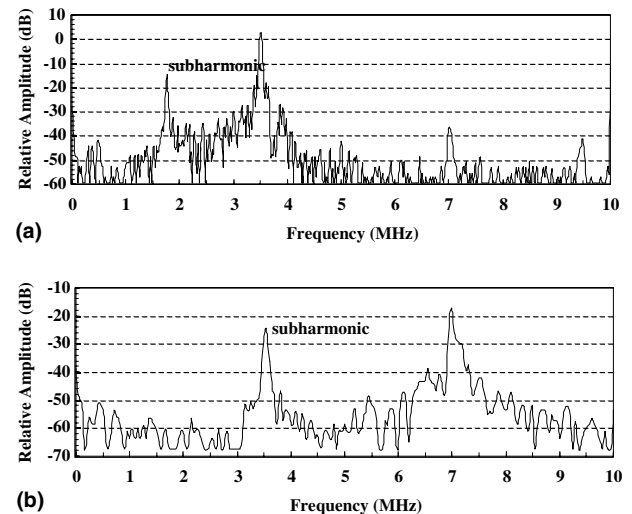


Fig. 6. Sonazoid spectra obtained using (a) the 3.5/1.75 MHz sub-arrays for transmission/reception and (b) the 7.0/3.5 MHz sub-arrays for transmission/reception (i.e., the MFHA is operating in SHI mode).

5. Discussion

Two novel ultrasound MFHA's for contrast enhanced HI and SHI have been designed and initial acoustic characterization have been performed. Each MFHA comprised of three co-linear sub-arrays of piezo-composite elements, one resonates at frequencies 2.5, 5.0 and 10.0 MHz, and the other at 1.75, 3.5, and 7.0 MHz. TRV's of 12–13 kPa/V were measured (at 1.0 mm) and RRS's (at the mechanical focus of 5.0 cm) were 5.1–8.8 mV/kPa (Table 3). Comparable transmitting and

receiving sensitivities exist in commercial transducer arrays [16]. The initial in vitro testing using Sonazoid demonstrated SNR's of up to 40 and 34 dB, respectively, in HI and SHI mode (Figs. 5 and 6). These SNR's are similar to those of regular B-mode imaging systems and better than scanners operating in HI mode [1].

The design of broadband transducer arrays can be systematically optimized utilizing the KLM model and an iterative approach, such as the statistically designed experiment method [18]. However, the resulting transducer array will still have a bandwidth less than one octave, where the design of the receiving filters is critical in minimizing harmonic interaction. The approach taken in this study is that the design of three separate arrays with different resonant frequencies provides added degrees of freedom in array design, permitting higher peak response and the ability to shape the adjacent sub-array spectral structures, thereby relaxing the design requirements of the receive filters.

One other transducer dedicated to nonlinear contrast imaging, a phased array, has been reported in the literature [19,20]. This array contains 96 elements operating at either 2.8 MHz with an 80% bandwidth (48 elements) or at 900 kHz with a 50% bandwidth (the remaining elements). The two different types of elements are arranged in an interleaved pattern (as odd and even) and can be controlled individually and separately. SNR's of over 30 dB were reported in HI mode [19]. While this array is capable of operating in SHI mode, no such results have been presented to date, but initial in vivo results in superharmonic mode are encouraging [20].

The preliminary experimental results on the MFHA's reported here will be used to produce a 96-element array design for clinical contrast imaging. The kerf width and filler will be chosen to place the spurious resonances of a given sub-array at the resonant frequencies of the adjacent sub-arrays. Each individual element will have an acoustically matched backing layer of tungsten-loaded epoxy to provide a minimum 30 dB absorption. They will also be tested for electro-acoustic parameters (including transmitting and receiving sensitivities). The goals are to hold the variation in element-to-element sensitivity to less than 2-dB and the cross-coupling on adjacent elements to at least -25 dB. Finally, the plan is to integrate the new MFHA with a commercial ultrasound scanner to perform in vitro and in vivo HI and SHI.

In conclusion, preliminary design and in vitro characterization of two MFHA's have been performed. They have an overall broad frequency bandwidth of at least two octaves. Due to the special design of the array assembly, the SNR for HI and SHI was comparable to that of regular B-mode and better than commercially available HI systems. However, further research on multi-element MFHA's is required before their potential for in vivo nonlinear contrast imaging can be assessed.

Acknowledgements

This work was supported by NIH grant no. 1 R43 RR14933-01.

References

- [1] B.B. Goldberg, J.S. Raichlen, F. Forsberg, *Ultrasound Contrast Agents: Basic Principles and Clinical Applications*, second ed., Martin Dunitz Ltd., London, 2001.
- [2] W. Lauterborne, Numerical investigation of nonlinear oscillations of gas bubble in liquids, *J. Acoust. Soc. Am.* 59 (1976) 283.
- [3] B.A. Schrope, V.L. Newhouse, Second harmonic ultrasound blood perfusion measurement, *Ultrasound Med. Biol.* 19 (1993) 567.
- [4] N. de Jong, R. Cornet, C.T. Lancee, Higher harmonics of vibrating gas-filled microspheres. Part one: Simulations, *Ultrasonics* 32 (1994) 447.
- [5] N. de Jong, R. Cornet, C.T. Lancee, Higher harmonics of vibrating gas-filled microspheres. Part two: Measurements, *Ultrasonics* 32 (1994) 455.
- [6] F. Forsberg, B.B. Goldberg, J.B. Liu, D.A. Merton, N.M. Rawool, On the feasibility of real-time, in vivo harmonic imaging with proteinaceous microspheres, *J. Ultrasound Med.* 15 (1996) 853.
- [7] P.M. Shankar, P.D. Krishna, V.L. Newhouse, Advantage of subharmonic over second harmonic backscatter for contrast-to-tissue echo enhancement, *Ultrasound Med. Biol.* 24 (1998) 395.
- [8] W.T. Shi, F. Forsberg, A.L. Hall, et al., Subharmonic imaging with microbubble contrast agents: initial results, *Ultrasonic Imaging* 21 (1999) 79.
- [9] F. Forsberg, W.T. Shi, B.B. Goldberg, Subharmonic imaging of contrast agents, *Ultrasonics* 38 (2000) 93.
- [10] G. Bhagavatheeshwaran, W.T. Shi, F. Forsberg, P.M. Shankar, Subharmonic generation from contrast agents in simulated neovessels, *Ultrasound Med Biol* 30 (2004) 199.
- [11] J. Chomas, P. Dayton, D. May, K. Ferrara, Nondestructive subharmonic imaging, *IEEE Trans. Ultrason Ferroelec. Freq. Contr.* 49 (2002) 883.
- [12] A. Bandyopadhyay, R.K. Panda, V.F. Janas, et al., Processing of piezocomposites by fused deposition technique, *J. Am Ceram. Soc.* 80 (1997) 1366.
- [13] A. Bandyopadhyay, R.K. Panda, T.F. McNulty, F. Mohammadi, S.C. Danforth, A. Safari, Piezoelectric ceramics and composites via rapid prototyping techniques, *Rapid Prototyping J.* 4 (1998) 37.
- [14] J. Souquet, P. Defranould, J. Desbois, Design of low-loss wide-band ultrasonic transducers for noninvasive medical application, *IEEE Trans. Sonics Ultrason* 26 (1979) 75.
- [15] B. Jadian, Design and development of a large area flexible array transducer for bone healing application, Ph.D. Thesis, Rutgers, The State University, New Brunswick, NJ, 1998.
- [16] X. Geng (Blatek Inc., State College, PA), R. Panda (Phillips Medical Systems, Andover, MA), Private communications, 2002.
- [17] P.C. Sontum, J. Østensen, K. Dyrstad, L. Hoff, Acoustic properties of NC100100 and their relation with the microbubble size distribution, *Invest. Radiol.* 34 (1999) 268.
- [18] R.E. McKeighen, Optimization of broadband transducer designs by use of statistical design of experiments, *IEEE Trans. Ultrason Ferroelec. Freq. Contr.* 43 (1996) 63.
- [19] A. Bouakaz, S. Frigstad, F.J. Ten Cate, N. De Jong, Super harmonic imaging: a new technique for improved contrast detection, *Ultrasound Med. Biol.* 28 (2002) 59.
- [20] A. Bouakaz, B.J. Krenning, W.B. Vletter, F.J. Ten Cate, N. De Jong, Contrast superharmonic imaging: a feasibility study, *Ultrasound Med. Biol.* 29 (2003) 547.